

The locally polar smectic A phase in V-shaped molecules

E-Joon Choi,^{*a} Eun-Chol Kim,^a Sang-Byung Park,^b Wang-Cheol Zin,^b You-Jin Lee^c and Jae-Hoon Kim^c

Received 15th August 2012, Accepted 1st October 2012

DOI: 10.1039/c2jm35530b

For focusing on the polar smectic A phase derived from the V-shaped molecules, bent-core molecules with an acute-angled central core (Ar = 1,2-phenylene or 2,3-naphthylene) and a lateral halogen substituent (X = F or Cl) were synthesized. Their mesomorphic properties were investigated by DSC, polarizing microscopy, X-ray and electro-optical measurements. We found that a compound with Ar/X = 2,3-naphthylene/Cl forms the conventional smectic A phase, whereas three compounds with Ar/X = 1,2-phenylene/F, 1,2-phenylene/Cl and 2,3-naphthylene/F form the locally polar smectic A phase (SmAP_R). According to our knowledge this is the first obvious experimental evidence that V-shaped molecules with an acute-subtended angled central core, in cooperation with a lateral halogen substituent, can form the SmAP_R.

1. Introduction

Nowadays the polar property of the mesophase is a hot issue in the research field of liquid crystals because of its potential application in advanced information-display areas of technology. In 1974, it was discovered that if chiral molecules with a rod-like mesogen form the tilted smectic phase their mesophases can possess the spontaneous polarization: these mesophases are the polar smectic C phase (SmCP).¹ In 1996, Takezoe and Watanabe's group reported the first obvious example of a SmCP derived from an achiral molecule with a bent-core mesogen.² In 1997, Clark and Walba's group depicted and explained the layer structure of the SmCP using three stereogenic elements such as chirality (+/−), clinacity (S/A) and polarity (F/A) of the adjacent layer: there are four states such as SmC_SP_A, SmC_AP_F, SmC_AP_A, and SmC_SP_F.³ Since then, a large number of studies have been made on the SmCP.

On the other hand, so far a limited number of studies on SmAP (the polar smectic A phase) have been reported.^{4–8} For an example, asymmetric banana-shaped molecules can form the SmAP_A.^{9,10} Recently, Pocięcha *et al.* have reported that SmAP in asymmetric banana-shaped molecules has a layered, nontilted, optically uniaxial and polarly ordered structure with a random direction of the layer polarization.¹¹ To account for the structure of such SmAP, five possible arrangements have been proposed, SmAP_F, SmAP_A, SmAP_α, SmAP₂, and SmAP_R: α stands for a

helicoidally modulated polarization with the short pitch; R stands for a randomly oriented polarization. Moreover, Shimbo *et al.* reported that such polar SmAP_F shows the fast polarization orientation and the associated birefringence as an in-plane electronic field was applied to vertically aligned cells, which originate from the cooperative motion of the bent molecules with a quasi-long-range order of dipoles based on a two-dimensional Langevin process.¹²

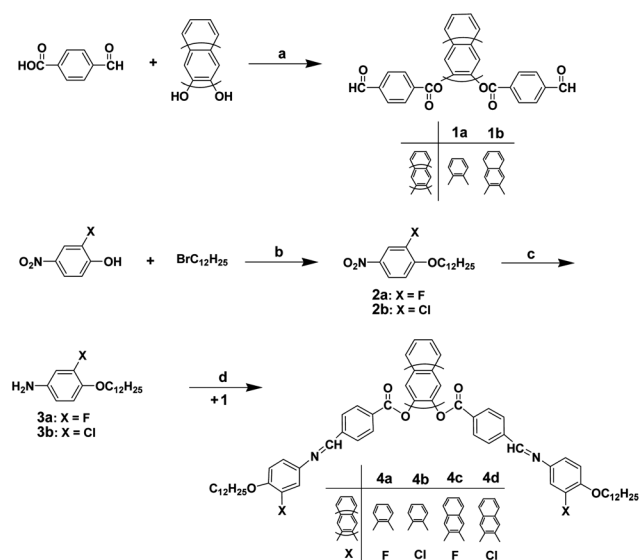
According to the bent angle of the central core, the bent-core molecules can be classified into two categories: the V-shaped molecules that have an acute angled central core and the banana-shaped molecules that have an obtuse angled central core. To date, the polar mesophase of the banana-shaped molecules has been an object of study for a long time. However, there is little agreement about the polar mesophase of the V-shaped molecules. At the beginning of 1990, Japanese groups first reported that the V-shaped molecules with a 1,2-phenylene central core form conventional nematic, smectic A and smectic B phases depending on the length of flexible terminals.^{13,14} Since then, more studies on this topic have been reported by several research groups. Prasad reported that a series of 1,2-phenylene bis[4-(4-alkoxyphenylazo)benzoates] form nematic, smectic A and crystal E phases.¹⁵ Yelamaggad *et al.* reported that V-shaped molecules with salicylaldehyde segments form nematic and smectic A phases due to the intramolecular hydrogen bonding.¹⁶ Watanabe *et al.* reported that V-shaped molecules with 1,2-, 1,3-, 1,7- and 2,3-dihydroxynaphthalene central cores form smectic A and B₄ phases.¹⁷ Recently, we reported that a main-chain polymer with a V-shaped mesogen based on 2,3-naphthalene forms SmCP_F¹⁸ and a V-shaped molecule with a 2,3-dihydroxynaphthalene central core forms an electric-field-induced SmAP.¹⁹

In this paper, four new V-shaped molecules with an acute-angled central core (Ar) and a lateral halogen substituent (X) have been synthesized as shown in Scheme 1. Their mesomorphic

^aDepartment of Polymer Science and Engineering, Kumoh National Institute of Technology, Gumi, Gyungbuk 730-701, Korea. E-mail: ejchoi@kumoh.ac.kr; Fax: +82 544787710; Tel: +82 544787684

^bDepartment of Material Science and Engineering, Pohang University of Science and Technology, Pohang, Gyungbuk 790-784, Korea

^cDepartment of Information Display Engineering, Department of Electronics and Communications Engineering, Hanyang University, Seoul, 133-701, Korea



Scheme 1 Synthetic route towards compounds: (a) DCC, DMAP, CHCl₃, rt, 24 h; (b) Na₂CO₃, DMF, reflux, 4 h; (c) 100 psi H₂, 10% Pd-C, EtOH, 70 °C, 4 h; (d) EtOH, 80 °C, reflux, 8 h.

properties were investigated by DSC, polarizing microscopy, X-ray diffraction, and electro-optical measurements. We have described the obvious experimental evidence that our V-shaped molecules can form the SmAP_R.

2. Experimental

2.1. Synthesis

The V-shaped molecules (**4a–4d**) were synthesized by a modification of the procedure previously reported by our group: compound **1** was prepared by the direct esterification,²⁰ and then compound **4** was prepared by nucleophilic addition followed by dehydration.¹⁸ The purity and the structure of the final compounds were confirmed by thin-layer chromatography, elemental analysis, and FT/IR and ¹H NMR spectrometry. The resultant data were in accordance with the expected formula.

Compound 4a. IR (KBr pellet, cm⁻¹): 3074 (aromatic =C–H, st), 2922, 2854 (aliphatic C–H, st), 1737 (C=O, st), 1512, 1488 (aromatic C=C, st), 1628 (C=N, st), 1242, 1106, 1070 (C–O, st). ¹H NMR (CF₃COOD, δ in ppm): 8.70 (2H, s, N=CH), 8.23–6.77 (16H, m, Ar–H), 4.02 (4H, t, *J* = 6.55 Hz, OCH₂), 1.84–1.66 (4H, m, OCH₂CH₂), 1.40–0.99 (36H, m, OCH₂CH₂CH₂). Elemental analysis calcd (%) for C₅₈H₇₀F₂N₂O₆: C 74.97, H 7.59, N 3.01; found C 75.13, H 7.89, N 3.21.

Compound 4b. IR (KBr pellet, cm⁻¹): 3063 (aromatic =C–H, st), 2923, 2850 (aliphatic C–H, st), 1738 (C=O, st), 1493, 1469 (aromatic C=C, st), 1617 (C=N, st), 1259, 1231, 1055 (C–O, st). ¹H NMR (CF₃COOD, δ in ppm): 8.44 (2H, s, N=CH), 8.23–6.74 (16H, m, Ar–H), 3.95–3.88 (4H, t, *J* = 6.54 Hz, OCH₂), 1.86–1.76 (4H, m, OCH₂CH₂), 1.43–1.25 (36H, m, OCH₂CH₂CH₂). Elemental analysis calcd (%) for C₅₈H₇₀Cl₂N₂O₆: C 72.41, H 7.33, N 2.91; found C 72.60, H 7.53, N 3.03.

Compound 4c. IR (KBr pellet, cm⁻¹): 3059 (aromatic =C–H, st), 2917, 2848 (aliphatic C–H, st), 1741 (C=O, st), 1519, 1462 (aromatic C=C, st), 1628 (C=N, st), 1272, 1102, 1013 (C–O, st). ¹H NMR (CF₃COOD, δ in ppm): 8.44 (2H, s, N=CH), 8.26–6.89 (18H, m, Ar–H), 4.06–3.99 (4H, t, *J* = 6.57 Hz, OCH₂), 1.85–1.74 (4H, m, OCH₂CH₂), 1.44–1.08 (36H, m, OCH₂CH₂CH₂). Elemental analysis calcd (%) for C₆₂H₇₂F₂N₂O₆: C 76.04, H 7.41, N 2.86; found C 76.13, H 7.60, N 2.90.

Compound 4d. IR (KBr pellet, cm⁻¹): 3062 (aromatic =C–H, st), 2922, 2851 (aliphatic C–H, st), 1734 (C=O, st), 1495, 1465 (aromatic C=C, st), 1617 (C=N, st), 1265, 1162, 1060 (C–O, st). ¹H NMR (CF₃COOD, δ in ppm): 8.43 (2H, s, N=CH), 8.25–6.72 (18H, m, Ar–H), 4.04–3.98 (4H, t, *J* = 6.39 Hz, OCH₂), 1.86–1.76 (4H, m, OCH₂CH₂), 1.44–1.25 (36H, m, OCH₂CH₂CH₂). Elemental analysis calcd (%) for C₆₂H₇₂Cl₂N₂O₆: C 73.57, H 7.17, N 2.77; found C 73.42, H 7.35, N 2.93.

2.2. Characterization

Instruments. IR and NMR spectra were obtained by a Jasco 300E FT/IR and a Bruker Avance 400 MHz NMR spectrometer, respectively. Elemental analysis was performed with a Thermo Scientific Flash 2000 Elemental Analyzer. The transition behaviors were characterized by a differential scanning calorimeter (Netzsch DSC 200 F3 Maia). DSC measurements were performed in a N₂ atmosphere with heating and cooling rates of 10 and 20 °C min⁻¹. Optical texture observation was carried out using a polarizing microscope (Carl Zeiss Axioskop 40 Pol) with a heating stage (Mettler FP82HT).

X-ray investigation. XRD measurements were performed in transmission mode with synchrotron radiation ($\lambda = 1.54 \text{ \AA}$) at the Pohang Accelerator Laboratory. When heating and cooling, the sample, which was sealed on both sides with a 7 μm thick Kapton film, was held in an aluminium sample holder. The data are presented as a function of $q = 4\pi\sin \theta/\lambda$ (θ : the scattering angle). The sample was heated with two cartridge heaters, and its temperature was monitored by a thermocouple placed close to the sample. A background scattering correction was performed by subtracting the scattering from the Kapton film.

Electro-optical measurement. The LC was injected between two ITO glass substrates by capillary action at 180 °C. Each non-patterned ITO glass substrate was spin-coated with a commercial planar alignment reagent (AL22620, JSR). The spin-coated alignment layer was pre-baked at 100 °C for 10 min to evaporate the solvent, and then cured at 210 °C for 1 hour to complete imidization reaction. The rubbing directions of the upper and the lower substrates were antiparallel to each other. The cell thickness was maintained using glass spacers of 4.5 μm. The temperature of the cell was maintained with an accuracy of within 0.1 °C using a heating stage (FP90, Mettler). The switching current response characteristics were measured by applying a triangle wave voltage ($E = 22 \text{ V } \mu\text{m}^{-1}$, $f = 3 \text{ Hz}$).

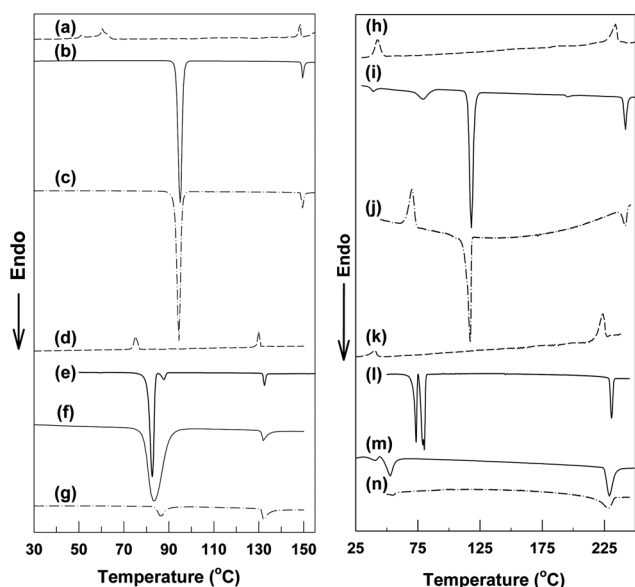


Fig. 1 DSC thermograms obtained with heating and cooling rates of 10 (a–d, f–i, k, m) or 20 °C min⁻¹ (e, j, l, n); dashed line: 1st cooling; solid line: 1st heating; dash-dotted line: 2nd heating. (a–c) **4a**; (d–g) **4b**; (h–j) **4c**; (k–n) **4d**.

3. Results and discussion

3.1. Mesogenic properties

Mesogenic properties have been examined by thermal, optical, and X-ray measurements. In Fig. 1, DSC thermograms of compounds show two distinctive transition temperatures that have been defined as melting (T_m) and isotropization (T_i) temperature, respectively. The transition temperatures and enthalpy changes defined by DSC are summarized in Table 1. Among four compounds, compound **4c** with Ar/X = 2,3-Naph/F shows the highest T_m value and compound **4d** with Ar/X = 2,3-Naph/Cl exhibits the lowest one. This implies that a highly bent 2,3-phenylene central core with a second ring extruded can play either a constructive or destructive role in molecular packing in the solid state in cooperation with the lateral halogen substituent. On the other hand, the ΔH_i values of compounds **4c** and **4d** are 2.5 and 3.6 times greater than those of compounds **4a** and **4b**, respectively. This means that the 2,3-naphthylene central core

Table 1 Transition temperatures (°C) and enthalpy changes (kJ mol⁻¹)

Compound	Ar/X	DSC scan ^a	T_m	ΔH_m	T_i	ΔH_i
4a	1,2-Phen/F	1-H	95	59.0	150	3.1
		1-C	61	7.3	148	3.1
		2-H	94	58.6	150	3.0
4b	1,2-Phen/Cl	1-H	83	54.9	133	2.6
		1-C	75	3.3	130	2.5
		2-H	88	3.0	133	2.5
4c	2,3-Naph/F	1-H	118	47.1	242	7.6
		1-C	42	6.4	234	6.1
4d	2,3-Naph/Cl	1-H	75	3.3	231	9.3
		1-C	41	2.5	224	7.1

^a Abbreviations: 1-H = 1st heating; 2-H = 2nd heating; 1-C = 1st cooling.

plays an important role in enhancing directional ordering of mesogens instead of steric hindrance in their mesophase.

In Fig. 1, the melting behavior of compound **4b** with X = Cl depends on the thermal history whereas compound **4a** with X = F did not show that. The fluorine atom can bestow better packing property due to higher electron negativity, lower molecular cohesive energy and smaller van der Waals radius compared with the chlorine atom. In the case of compounds **4c** and **4d**, the similar result was observed although their T_i s are high enough to suffer from thermal decomposition (Fig. 1j and n).

Fig. 2 shows the X-ray diffraction patterns obtained during heating and cooling processes. The powder samples were mounted between two amorphous Kapton films. At temperatures below T_m defined by DSC, all compounds exhibited many diffraction peaks, indicating a crystalline state. When heated above the T_m , a strong peak was found in the small angle region, while all peaks in the wide-angle region disappeared. This is indicative of the smectic phase. When further heated above T_i defined by DSC, only broad scattering patterns were observed, indicating an isotropic liquid phase. Subsequently, when the isotropic liquid was cooled below the T_i , the smectic phase appeared reversibly in all compounds. When further cooled to room temperature, compound **4a** exhibited most distinctive recrystallization, according to the DSC result.

In Table 2, the layer spacing (d) values of the smectic mesophases are in the range of 3.77–4.00 nm. In general the d -spacing values show subtle differences not only depending on the structure but also on the temperature. This indicates that bent angles of molecules can be altered by changing the temperature in the melt state.

To account for a stable conformation, in a similar way with a 1,3-phenylene central unit,^{21,22} we have postulated that phenyl rings are coplanar when carbonyl groups are attached to them, and alkyloxy groups in all-*trans* conformation are equiplanar to the benzene rings. Moreover, we assumed that the bent angle is 60 degrees and there is no intercalation between chains. Then, we can estimate the length of the molecule with the all-*trans*-conformation to be 3.53 nm by using the PCFF force-field model of martial studio. However, this value is not matched with d values determined by X-ray measurements. Nevertheless, the postulation that the molecules would form a tilted smectic mesophase can be excluded because the d -spacing value would be smaller than 3.53 nm. In the mean time, if we assume that bent angles are larger than 60°, the fact that d -values are larger than 3.53 nm can be explained by the formation of the smectic A phase. Then, we can calculate the opening angle of arms to be 76.9–82.6 degrees corresponding to $d = 3.77$ –4.00 nm.

Fig. 3 shows cross-polarizing optical micrographs obtained by using a normal slide glass. During the heating process, compounds **4a** and **4d** showed the optical texture shown in Fig. 3a and b, respectively, while compounds **4b** and **4c** showed a homeotropic-like optical texture. When the isotropic liquid was cooled, no birefringence occurred at the isotropic-to-smectic transition temperatures and then the smectic phases held a homeotropic optical texture until solidification. Note that compounds **4a** and **4c** showed the Maltese-cross spherulites with a homeotropic region as shown in Fig. 3c and d, respectively.

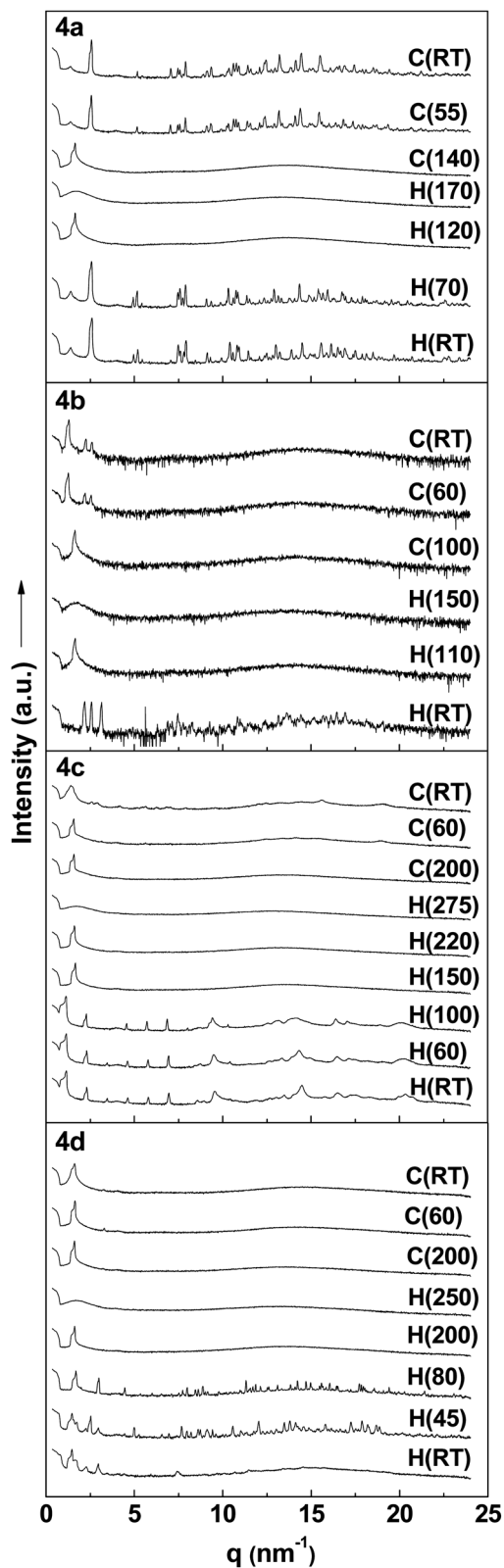


Fig. 2 Synchrotron radiation X-ray diffraction profiles of compounds obtained at given temperatures ($^{\circ}\text{C}$, in parentheses). Abbreviations: RT = room temperature; H = heating process; C = cooling process.

Table 2 The q -value (q) and layer spacing (d) for smectic phases

Compound	Ar/X	Process temp. ^a ($^{\circ}\text{C}$)	q (nm^{-1})	d (nm)
4a	1,2-Phen/F	H(120)	1.64	3.83
		C(140)	1.64	3.83
4b	1,2-Phen/Cl	H(110)	1.65	3.80
		C(100)	1.64	3.83
4c	2,3-Naph/F	H(150)	1.67	3.77
		H(220)	1.61	3.90
		C(200)	1.58	3.97
		C(60)	1.57	4.00
4d	2,3-Naph/Cl	H(200)	1.62	3.87
		C(200)	1.61	3.90
		C(60)	1.64	3.83

^a Heating (H) and cooling (C) process temps. are given in parentheses.

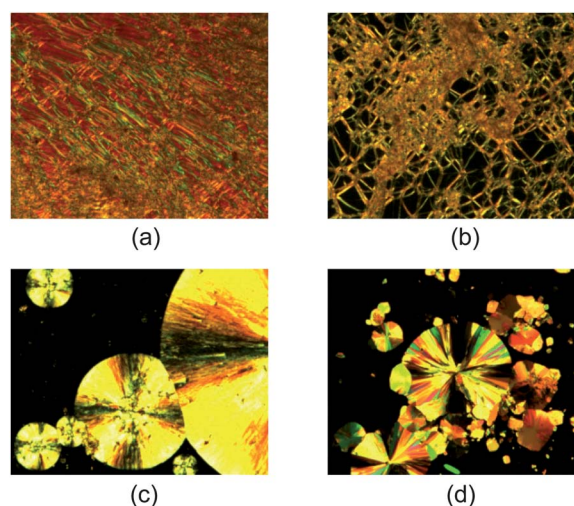


Fig. 3 Cross-polarizing optical micrographs obtained at given temperature ($\times 200$). On heating: (a) 4a, at 127°C ; (b) 4d, at 225°C . On cooling: (c) 4a, at 37°C ; (d) 4c, at 65°C .

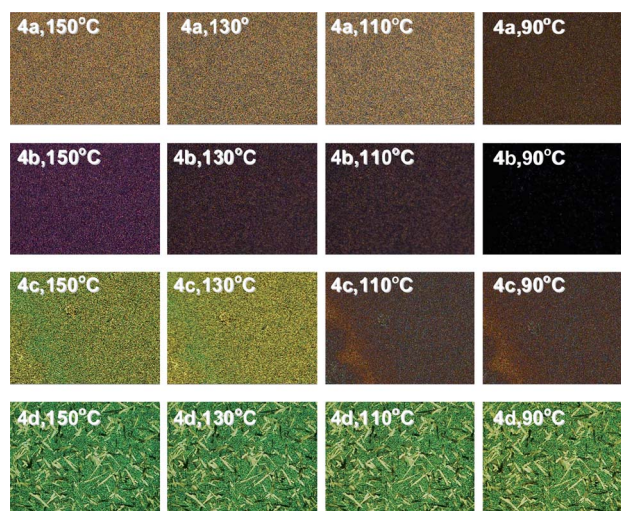


Fig. 4 Cross-polarized optical micrographs obtained using planarly aligned cells at given temperatures.

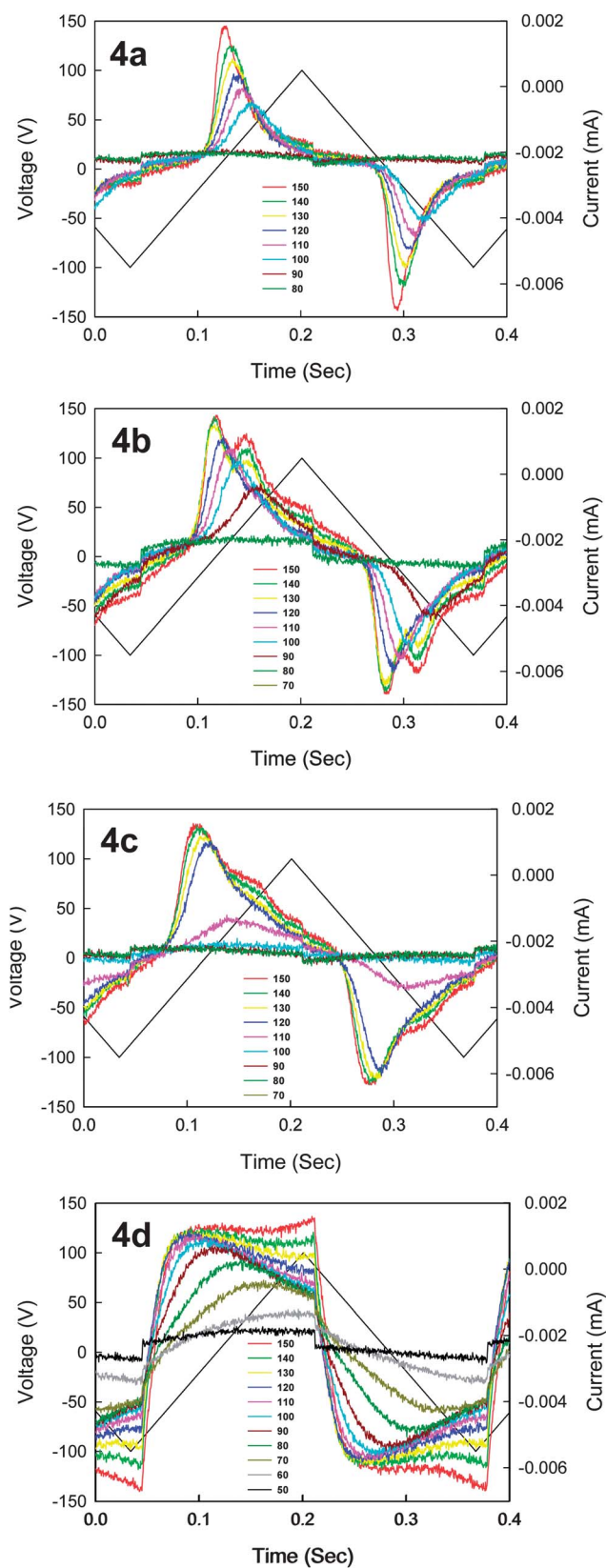


Fig. 5 Switching current response for compounds by applying a triangular voltage ($E = 22 \text{ V } \mu\text{m}^{-1}$, $f = 3 \text{ Hz}$) at given temperatures.

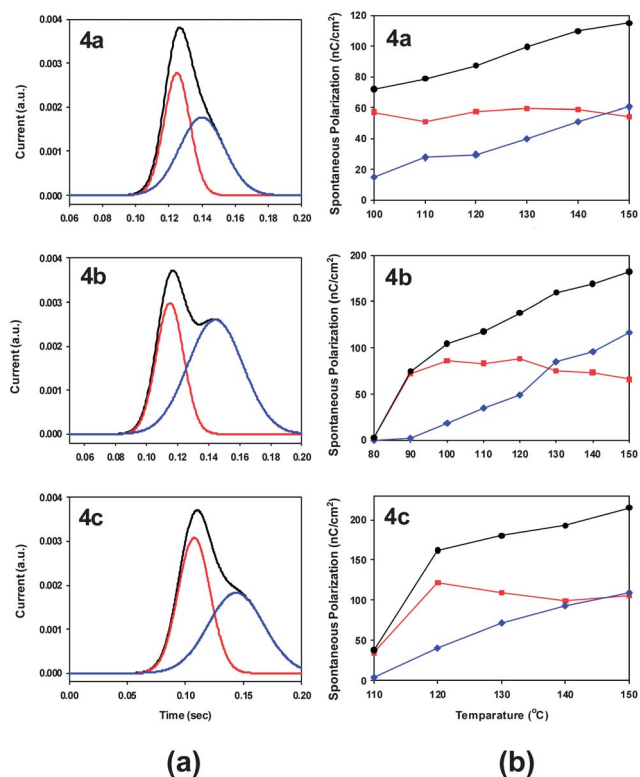


Fig. 6 (a) Peak separations of reverse current curves taken at the smectic phase. (b) Temperature dependence of the polarization estimated from the 1st peak (■), 2nd peak (◆), and total peak (●) of reverse current.

3.2. Electro-optical property

For electro-optical investigation, planarly aligned cells were used. The rubbing directions of the upper and the lower substrates were antiparallel to each other. In Fig. 4, the directions of a polarizer (P) and an analyzer (A) crossing each other make an angle of 45° with the rubbing direction (R). On the planar alignment layers, the optical textures of compounds **4a–4c** show the incomplete unidirectional alignment similar to micro-domains. The transmittance differences among these compounds are attributed to the different effective retardation: although the cell gaps are almost the same, the incomplete uniformity in alignment and the different magnitude of birefringence can lead each texture to different brightness and colors. Nonetheless, compound **4d** has a totally different texture compared with compounds **4a–4c**. This indicates that the former forms a different type of smectic phase from the latter.

Moreover, we have investigated the polar property of these smectic mesophases using current peak evaluation. Fig. 5 shows the switching current response on applying a triangular voltage. The reverse current peaks appeared at every half period of applied voltage, indicating a polar switching. In Fig. 6a, all the reverse current peaks are clearly separated by two individual peak functions. In Fig. 6b, the spontaneous polarizations gradually increase as the temperature increases. As a result, we have suggested that the smectic phases of **4a–4c** are locally polar, SmAP_R . But the smectic phase of **4d** is conventional.

4. Conclusions

Four V-shaped molecules containing an acute-angled central core (Ar = 1,2-Phen or 2,3-Naph) and a lateral halogen substituent (X = F or Cl) have been synthesized. Their mesomorphic properties were investigated by DSC, polarizing microscopy, X-ray and electro-optical measurements. All compounds were enantiotropically liquid crystalline. In general, compounds showed homeotropic optical textures using a normal slide glass without surface treatment. In contrast, using a planar alignment cell, compounds with Ar/X = 1,2-Phen/F, 1,2-Phen/Cl, and 2,3-Naph/F showed optical textures with incomplete unidirectional alignment. According to our experimental data, we have concluded that compounds with Ar/X = 1,2-Phen/F, 1,2-Phen/Cl, and 2,3-Naph/F formed the locally polar smectic A phase, SmAP_R. But compound with Ar/X = 2,3-Naph/Cl formed the conventional smectic A phase. From the structural point of view, the smectic A phase in these compounds can be compared with the smectic C phase¹⁸ in the polymer analogues. This different mesomorphism may be attributed to competition between mesogenic unit's tendency toward molecular ordering and main chain's tendency toward stable conformation, which is much greater in the melt state of the polymer than that of the compound. Meanwhile it is not clear why **4d** formed the conventional A phase while the other compounds formed the polar smectic A phase. Perhaps the lateral chlorine substitution is less effective to the dipolar orientation than the lateral fluorine substituent. Further study is needed to fully understand this subject.

Acknowledgements

This work was supported by the National Research Foundation of Korea (KOSEF) grant funded by Korea government (MEST) (no. R01-2008-000-11521-0). This work was supported in part by KRCF (Korea Research Council of Fundamental Science & Technology) and KIST (Korea Institute of Science and Technology) for NAP (National Agenda Project) program, and supported in part by KIST internal project.

References

- 1 R. B. Meyer, L. Liebert, L. Strzelecki and P. Keller, *J. Phys. Lett.*, 1975, **36**, L69.
- 2 T. Niori, T. Sekine, J. Watanabe, T. Furukawa and H. Takezoe, *J. Mater. Chem.*, 1996, **6**, 1231.
- 3 D. R. Link, G. Natale, R. Shao, J. E. MacLennan, N. A. Clark, E. Körblova and D. M. Walba, *Science*, 1997, **278**, 1924.
- 4 H. R. Brand, P. E. Cladis and H. Pleiner, *Macromolecules*, 1992, **25**, 7223.
- 5 B. K. Sadashiva, R. A. Reddy, R. Pratibha and N. V. Madhusudana, *J. Mater. Chem.*, 2002, **12**, 943.
- 6 H. N. S. Murthy and B. K. Sadashiva, *Liq. Cryst.*, 2004, **31**, 567.
- 7 S. T. Wang, S. F. Han, A. Cady, Z. Q. Liu, A. Kamenev, L. Glazman, B. K. Sadashiva, R. A. Reddy and C. C. Huang, *Phys. Rev.*, 2004, **70**, 061705.
- 8 R. A. Reddy and B. K. Sadashiva, *J. Mater. Chem.*, 2004, **14**, 310.
- 9 (a) A. Eremin, S. Diele, G. Pelzl, H. Nádasi, W. Weissflog, J. Salfetnikova and H. Kresse, *Phys. Rev.*, 2001, **64**, 051707; (b) M. W. Schröder, S. Diele, N. Pancenko, W. Weissflog and G. Pelzl, *J. Mater. Chem.*, 2002, **12**, 1331.
- 10 (a) C. Keith, M. Prehm, Y. P. Panarin, J. K. Vij and C. Tschierske, *Chem. Commun.*, 2010, **46**, 3702; (b) Y. P. Panarin, M. Nagaraj, J. K. Vij, C. Keith and C. Tschierske, *EPL*, 2010, **92**, 26002; (c) M. Nagaraj, Y. P. Panarin, J. K. Vij, C. Keith and C. Tschierske, *Appl. Phys. Lett.*, 2010, **97**, 213505.
- 11 D. Pocięcha, M. Čepić, E. Gorecka and J. Mieczkowski, *Phys. Rev.*, 2003, **91**, 185501.
- 12 Y. Shimbo, Y. Takanishi, K. Ishikawa, E. Gorecka, D. Pocięcha, J. Mieczkowski, K. Gomola and H. Takezoe, *Jpn. J. Appl. Phys.*, 2006, **45**, 282.
- 13 M. Kuboshita, Y. Matsunaga and H. Matsuzaki, *Mol. Cryst. Liq. Cryst.*, 1991, **199**, 319.
- 14 H. Matsuzaki and Y. Matsunaga, *Liq. Cryst.*, 1993, **14**, 105.
- 15 V. Prasad, *Liq. Cryst.*, 2001, **28**, 145.
- 16 C. V. Yelamagga, I. Shashikala, D. S. Rao and S. K. Prasad, *Liq. Cryst.*, 2004, **31**, 1027.
- 17 S. K. Lee, Y. Naito, L. Shi, M. Tokita, H. Takezoe and J. Watanabe, *Liq. Cryst.*, 2007, **34**, 935.
- 18 E.-J. Choi, E.-C. Kim, C.-W. Ohk, W.-C. Zin, J.-H. Lee and T.-K. Lim, *Macromolecules*, 2010, **43**, 2865.
- 19 E.-J. Choi, X. Cui, C.-W. Ohk, W.-C. Zin, J.-H. Lee, T.-K. Lim and W.-G. Jang, *J. Mater. Chem.*, 2010, **20**, 3743.
- 20 E.-J. Choi, X. Cui, W.-C. Zin, C.-W. Ohk, T.-K. Lim and J.-H. Lee, *ChemPhysChem*, 2007, **8**, 1919.
- 21 K. Fodor-Csorba, A. Vajda, G. Galli, A. Jákli, D. Demus, S. Holly and E. Gács-Baiz, *Macromol. Chem. Phys.*, 2002, **203**, 1556.
- 22 W. Weissflog, Ch. Lischka, S. Diele, G. Pelzl, I. Wirth, S. Grande, H. Kresse, H. Schmalfuss, H. Hartung and A. Stettler, *Mol. Cryst. Liq. Cryst.*, 1999, **333**, 203.